Nanoliposomes co-encapsulating a CT imaging contrast agent and photosensitizer for enhanced, imaging guided photodynamic therapy of cancer

Hao Xu[1, 2], Tymish Y. Ohulchanskyy[1,*], Artem Yakovliev[1], Roman Zinyuk[1], Jun Song[1], Liwei Liu[1], Junle Qu[1,*], Zhen Yuan[2,*]

1. Key Laboratory of Optoelectronic Devices and Systems of Ministry of Education and Guangdong Province, College of Optoelectronic Engineering, Shenzhen University, Shenzhen, Guangdong 518060, P.R.China
2. Bioimaging Core, Faculty of Health Sciences, University of Macau, Avenida da Universidade, Taipa, Macau SAR 999078, P.R.China

*Corresponding authors: tyo@szu.edu.cn, jlqu@szu.edu.cn, zhenyuan@umac.mo

Supplementary material

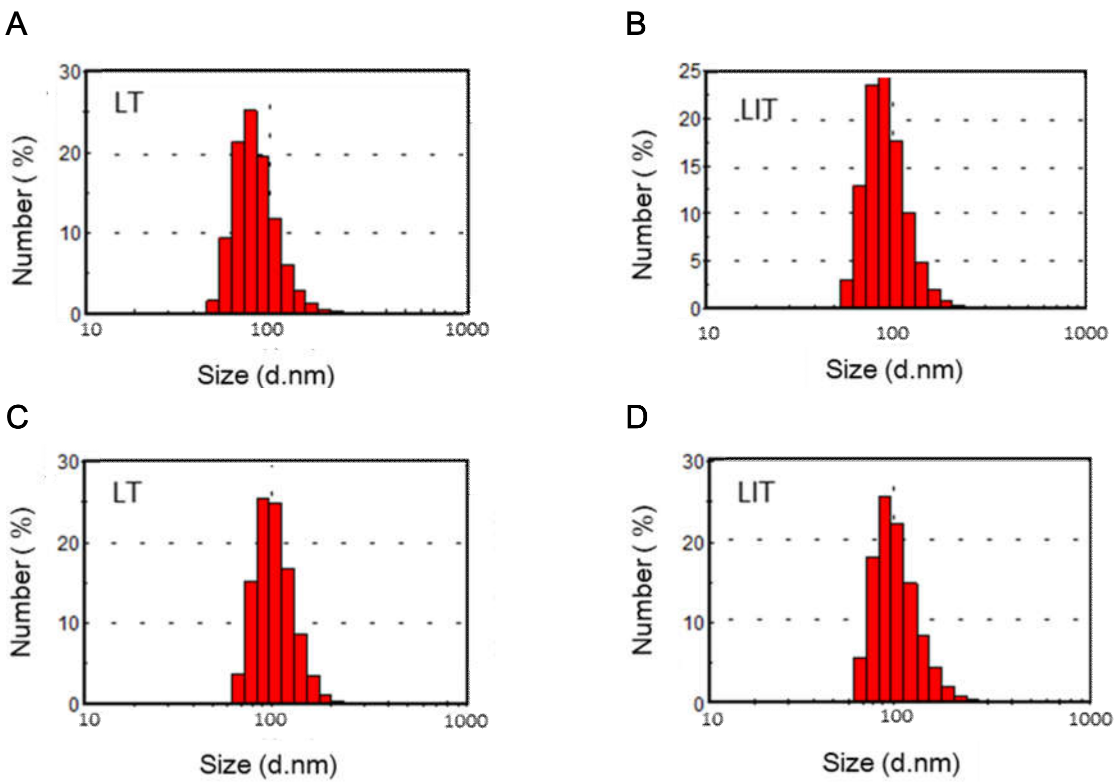

Figure S1. Size distribution of liposomal nanoformulations. (A) NL encapsulating $TPPS_4$ ((LT) after preparation; (B) NL co-encapsulating iodixanol and $TPPS_4$ (LIT) after preparation; (C) LT after 40 days of storage. (d) LIT after 40 days of storage.

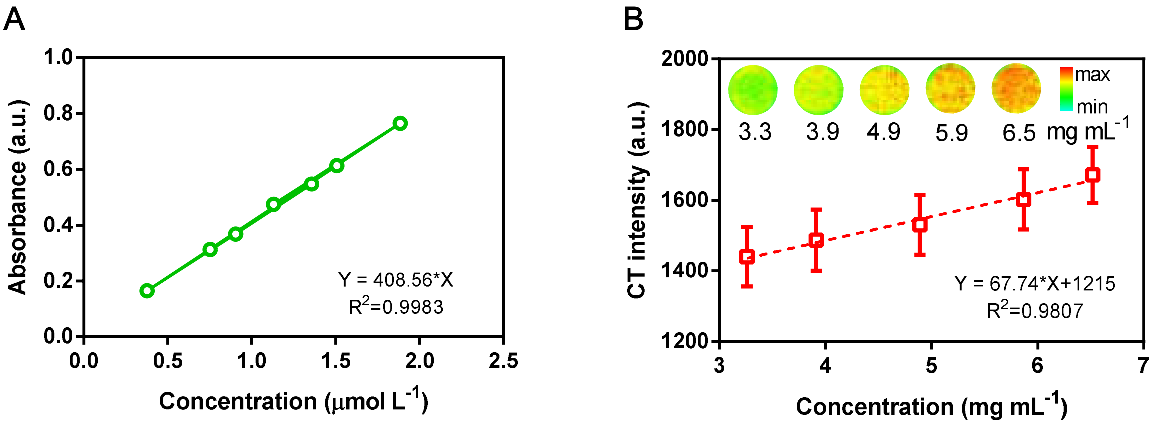

Figure S2. (A) Concentration dependence of $TPPS_4$ absorbance at 420 nm. (B) Phantom images and CT intensity measurements of iodixanol.

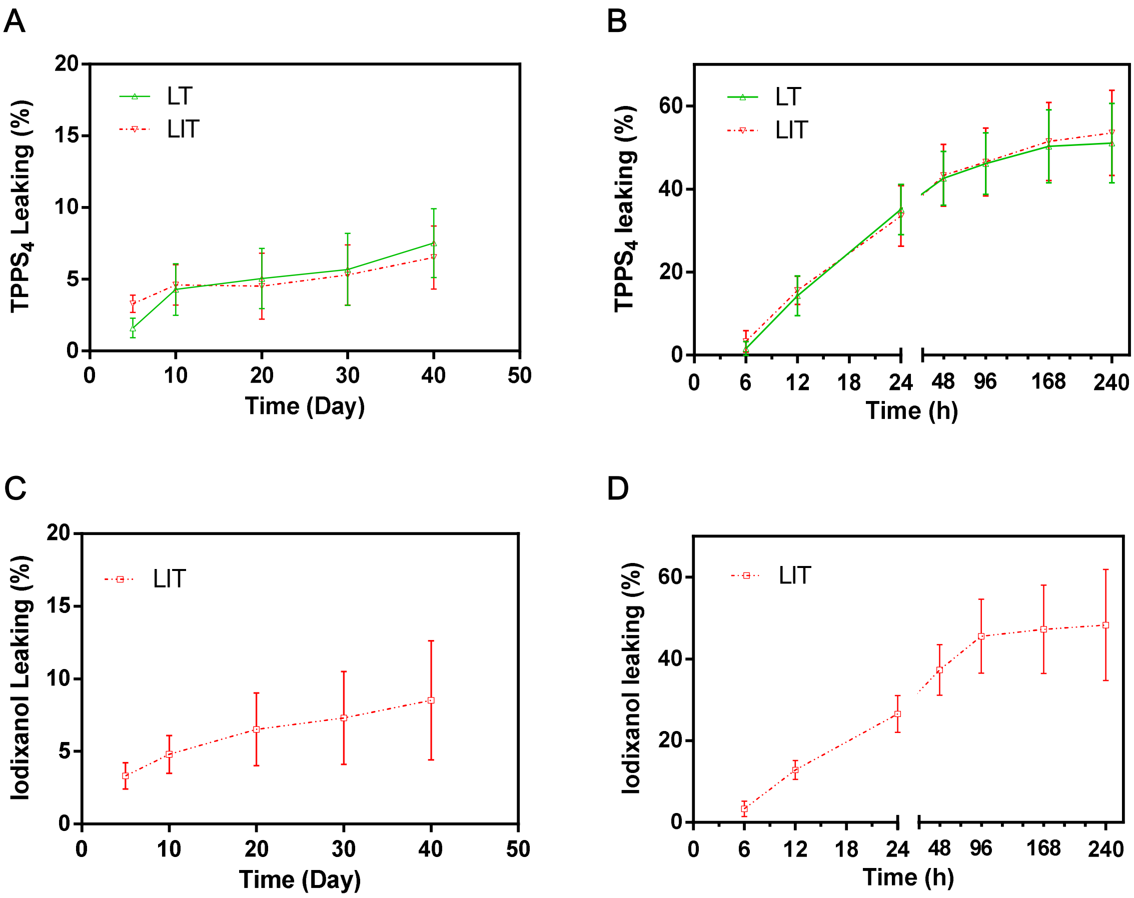

Figure S3. Monitoring the regent leakage from the prepared CPNL at different storage conditions. (A) $TPPS_4$ leakage from LT and LIT (in PBS at 4 °C); (B) $TPPS_4$ leakage from LT and LIT (in PBS with 10% FBS at 37 °C); (C) Iodixanol leakage from LIT(in PBS at 4 °C); (D) Iodixanol leakage from LIT (in PBS with 10% FBS at 37 °C).

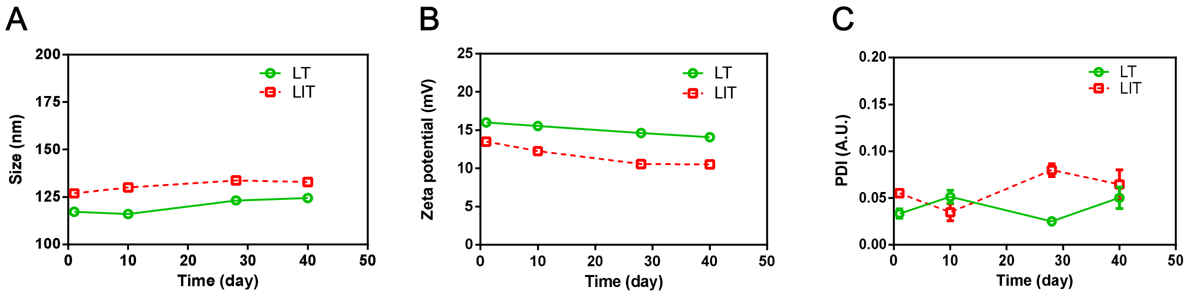

Figure S4. Monitoring the storage stability of size (A), zeta potential (B) and PDI (C) for the prepared NL at the storage conditions (in PBS at 4 ℃).

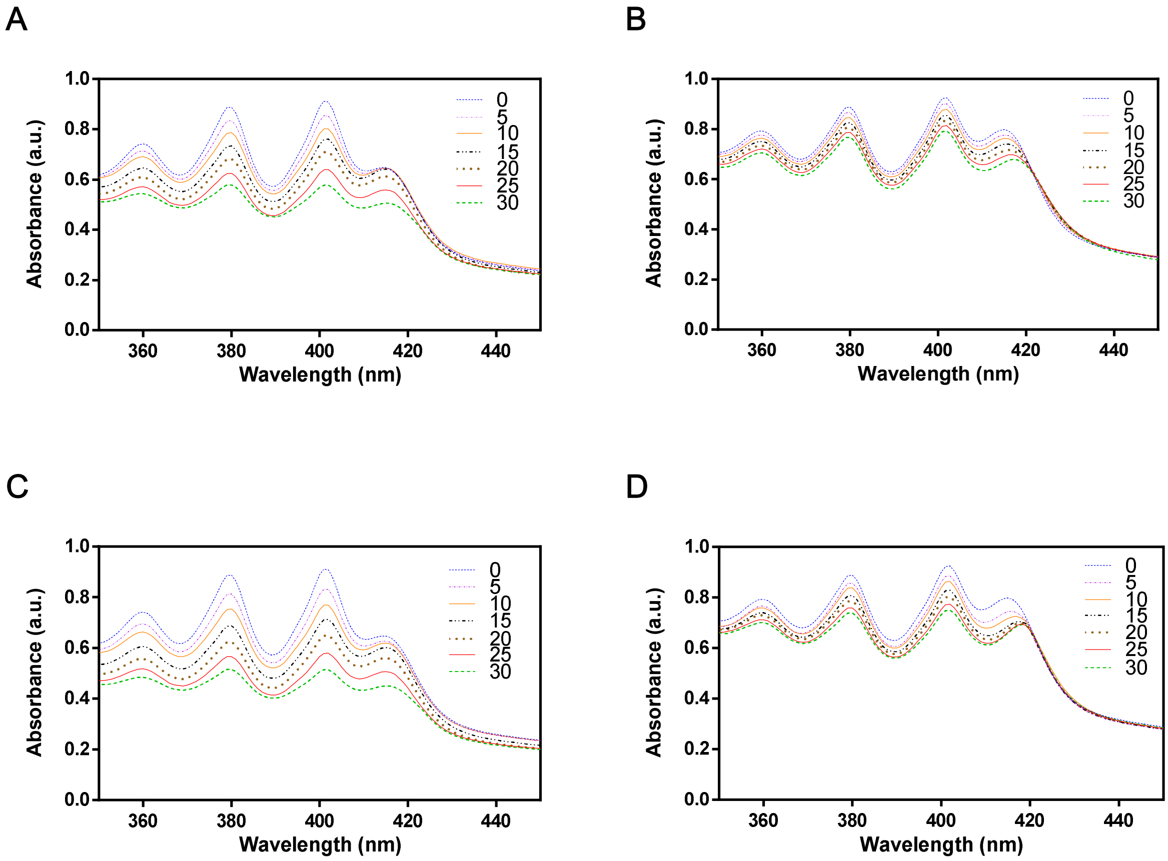

Figure S5. Absorption spectra of ABDA in water suspensions of $TPPS_4$ nanoformulations under 552 nm and 640 nm laser irradiation. Samples were irradiated at laser power density of 50 mW·cm^{-2} for 0, 5, 10, 15, 20, 25 and 30 min. (A) ABDA in LIT suspension under 640 nm laser irradiation; (B) ABDA in LT suspension under 640 nm laser irradiation; (C) ABDA in LIT suspension under 552 nm laser irradiation; (D) ABDA in LT suspension under 552 nm laser irradiation.

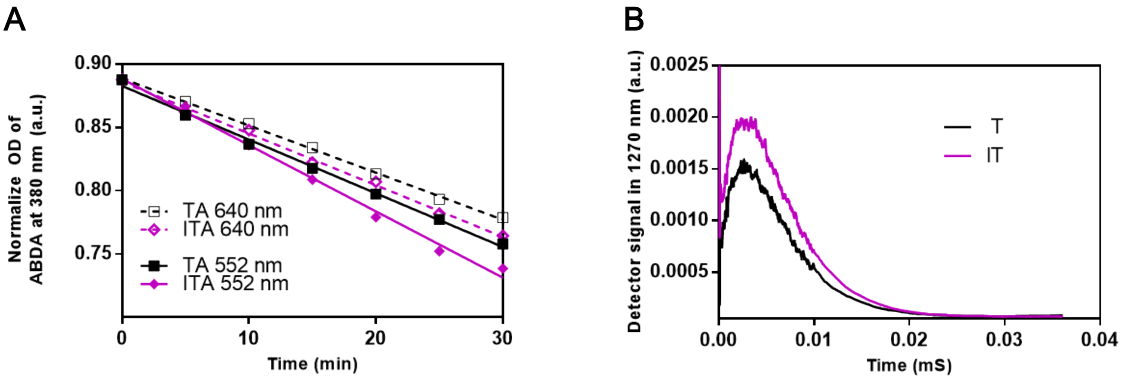

Figure S6. (A) Comparison of ABDA bleaching as a measure of the singlet oxygen generation in $TPPS_4$ solution (TA) and $TPPS_4$ solution win presence of iodixanol (ITA). (B) Decays of singlet oxygen phosphorescence at 1270 nm illustrating the singlet oxygen generation by free $TPPS_4$ in presence iodixanol (IT) and without it (T). PBS solutions, concentration of $TPPS_4$ C_{TPPS4}=8 µM, concentration of iodixanol $C_{Iodixanol}$=7 mM.

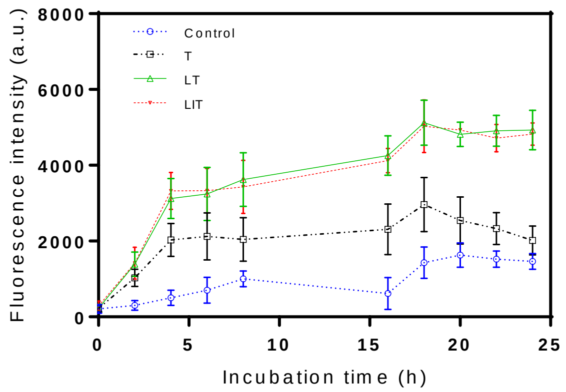

Figure S7. Cellular uptake of $TPPS_4$ in different formulations (free T, LT and LIT) at different incubation times. Control shows background (level of autofulorescence), when no fluorescent $TPPS_4$ was added to the cells.

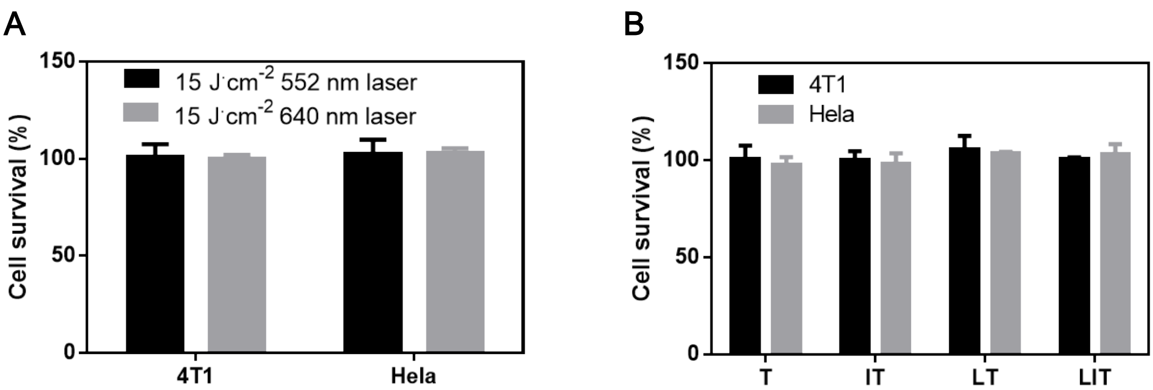

Figure S8. Cell viability assay performed 24 hours after treatment or irradiation. (A) irradiation with 552 nm and 640 nm lasers at the same irradiation dose (15 J cm^{-2}) in absense of $TPPS_4$; (B) 4T1 and Hela cells viability in response to the dark treatment with 40 µM of different formulations of $TPPS_4$ (i.e., free $TPPS_4$, IT, LT or LIT).

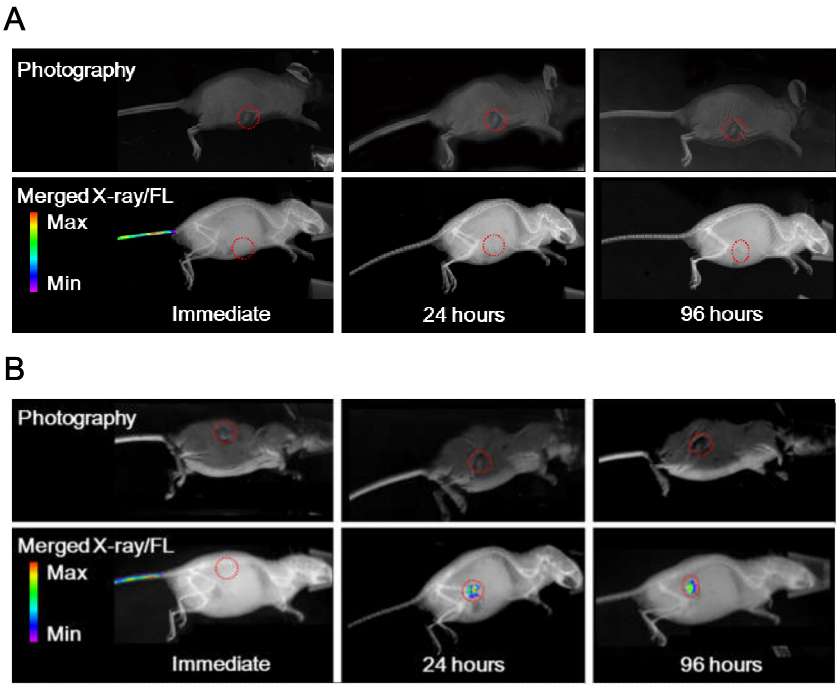

Figure S9. Photography and X-ray/fluorescence (X-ray/FL) images of the tumored nude mouse at various time points (2, 24, 96 h) post injection with (A) free $TPPS_4$ and (B) liposomal $TPPS_4$ (LT). Tumor location is shown with red circle.

Figure S10. Photography images of the tumored nude mice before and 30 days after treatment with different formulations and irradiation.

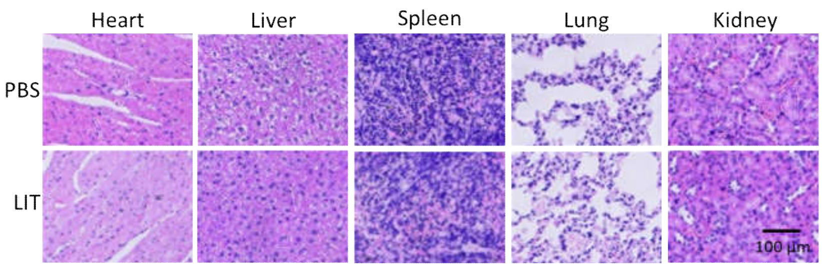

Figure S11. Histological sections of heart, liver, spleen, lungs, and kidney samples, collected after 7 days post injection with LIT formulation (lower row) and PBS (upper row). Sections were stained with H&E and observed under a light microscope.